Acta Biologica Szegediensis

Volume 64(2):239-249, 2020
Acta Biologica Szegediensis
http://abs.bibl.u-szeged.hu/index.php/abs

DOI:10.14232/abs.2020.2.239-249

ARTICLE

Potentials of synthesised *Lessertia montana* zinc oxide nanoparticles on free radicals-mediated oxidative stress and carbohydrate-hydrolysing enzymes

Fatai O. Balogun, Anofi O.T. Ashafa*

Phytomedicine and Phytopharmacology Research Group, Department of Plant Sciences, University of the Free State, Phuthadijthaba 9866, Qwaqwa, Free State, South Africa

ABSTRACT The study evaluated the effects of green absorbed zinc oxide nanostructures on oxidative stress-mediated free radicals and carbohydrate-hydrolysing enzymes. The synthesised *Lessertia montana* zinc oxide nanoparticles were characterised using different spectroscopic, microscopic, and diffraction techniques. The activity of *L. montana* ZnONPs against 1,1-diphenyl-2-picrylhydrazyl (DPPH), 2,2'-azino-bis(3-ethylbenzothiazoline-6-sulfonic acid (ABTS), metal chelating assay, alpha-amylase and alpha-glucosidase were determined using standard methods. *L. montana* ZnONPs were stable nanoparticles (NPs), appeared cubical (predominantly) in shape, and in nanometre range sizes. The synthesised NPs are very active ($p < 0.05$) against DPPH and alpha-glucosidase (0.120 and 0.037 g/L, respectively) when compared with other samples and controls, quercetin (0.349 g/L) and acarbose (0.065 g/L). However, their interaction with quercetin revealed a good ABTS (0.093 g/L) scavenging and an excellent metal chelating (0.027 g/L) effect compared to other samples. The mode of inhibition of alpha-amylase and alpha-glucosidase enzymes by *L. montana* ZnONPs was competitive and non-competitive, respectively. The study outcomes revealed that the synthesised ZnONPs possessed the potential to mitigate oxidative stress and diabetes *in vitro*.

Acta Biol Szeged 64(2):239-249 (2020)

KEY WORDS
antidiabetics
FTIR
green synthesis
Lessertia montana
nanoparticles
zinc oxide

ARTICLE INFORMATION
Submitted
18 October 2020.
Accepted
02 November 2020.
***Corresponding author**
E-mail: ashafaaot@ufs.ac.za

INTRODUCTION

Nanoparticles (NPs) owing to excellent features have continued to find relevance in different scientific domains such as medicine, food, cosmetics, textiles, etc. based on their size, distribution, and morphology (Sorescu et al. 2016). They are very important because of the atom-like characteristics resulting from a large surface area to volume ratio among many others (Nithya and Kalyanasundharam 2019). Nanostructures, (NS) be it metallic (gold, silver, platinum, zinc, etc.) or their corresponding oxides such as zinc oxide are synthesised via physical, chemical, and biological methods. However, due to side effects resulting from chemical synthesis involving the use of dangerous chemicals leading to the release or production of environmentally unfriendly by-products, interest in an eco-friendly method found in biological procedures becomes germane (Ogunyemi et al. 2019).

The use of medicinal plants in the biosynthesis of NPs is a laudable and/ or better alternative aimed or embraced for the production of safe NS devoid of toxic substances. The reason for the medicinal plant usage or exploration has been attributed to the presence of functional groups arising from the inherent phytoconstituents such as phenols, flavonoids, alkaloids, amide, amine, terpenoids, etc. (Rai and Ingle 2012; Ogunyemi et al. 2019)

Zinc oxide, a metallic oxide NP, classed with the likes of Au, C, and graphene is regarded as a superior NS as a result of its wide and numerous applications in electronics, biology, medicine, communication, etc. In fact, immense progress on the use or application of this NP has continued to be felt particularly in the area of gene delivery, biological identification/labelling, drug development/delivery, biological sensor, nanomedicine, optical/ chemical properties and so on. Additionally, the recent trend in the use of natural products in the synthesis of NPs had also been explored with ZnO. It is therefore interesting to note that quite a number of plants including but not limited to *Aloe barbadensis*, *Abutilon indicum*, *Solanum torvum*, *Laurus nobilis*, *Olea europaea*, *Hibiscus subdariffa*, *C. halicabum*, *Costus igneus*, etc. have found their relevance as used in the ZnONPs synthesis (Sangeetha et al. 2011; Bala et al. 2015; Nithya and Kalyanasundharam 2019; Prashanth et al. 2018; Ezealisiji et al. 2019; Fakhari et al. 2019; Ogunyemi et al. 2019; Vinotha et al. 2019) with

established antibacterial, antioxidant and antidiabetic effects. Additionally, in the review compiled by Vishnukumar and others (2018), it was evident that the part of plants mostly studied for ZnONPs applications is their leaves. Notwithstanding the afore-mentioned, very few reports are available in the literature on the antioxidative and antidiabetic effects of plant synthesised ZnONPs (Vishnukumar et al. 2018).

It is interesting to state that quite a number of studies centred on modifying the processes involved in the synthesis of zinc oxide nanoparticles have been reported by various authors as cited in the work of Vishnukumar et al. (2018), these modifications were in an effort to establish methods with better potentials of the NPs. While some reports studied the impact of varying concentrations, different solvents (during synthesis), temperature, etc. on the crystallite size of the synthesised nanoparticles, others investigated the need to maintain the pH using NaOH to enhance the precipitation kinetics. To a very large extent, high concentration and temperature are opined to bring about a reduction in the (crystallite) size of the NPs while a NaOH mediated synthesis presented a larger size NS as witnessed in a study using *Coriandrum sativum* leaf extract.

In terms of application and/ or biomedical advancement of phyto-synthesised ZnONPs, efforts on a number of plants had culminated into huge successes in diseases management (against free radical, cancer, bacterial and fungal infections, etc.), drug development, cosmetics, optical devices, solar cells, etc. (Vishnukumar et al. 2018).

Lessertia montana (previously *Sutherlandia montana*), a member of the Fabaceae family is a South African indigenous plant whose ethnobotanical attributes and indigenous uses were well reported in the work of Ashafa et al. (2019). The pharmacological potentials of the leaf and whole plant as an anticancer, anti-stress, antidepressant, anti-HIV, antioxidant and antidiabetic are adequately submitted in the different reports and/ or reviews (van Wyk and Albrecht 2008; Aboyade et al. 2014). In fact, the phytochemical determination, antioxidative and antidiabetic properties of the seeds, pods and leaf extracts of the plant were evaluated in our laboratory (Alimi and Ashafa, 2018; Ashafa et al. 2019) and these studies revealed the superior pharmacological benefits of the leaves than other parts. Hence, this study was designed to investigate the antioxidant and antidiabetic potentials (*in vitro*) of zinc oxide nanoparticles synthesised from *L. montana*.

MATERIALS AND METHODS

Chemicals

Acarbose, quercetin, p-nitrophenyl-α-D-glucopyranoside (pNPG), porcine pancreatic α-amylase, rat intestinal α-glucosidase, 1, 1-diphenyl-2-picrylhydrazyl (DPPH) and 2, 2′-Azino-bis(3-ethylbenzothiazoline-6-sulfonic acid (ABTS) were purchased from Sigma-Aldrich (South Africa) while zinc oxide was obtained from Merck Chemicals (South Africa). The water used was glass distilled while other chemicals/reagents used were of analytical grade.

Preparation of plant extracts

The whole plant of *Lessertia montana* was collected in Kestell, eastern Free State, South Africa. It was identified and authenticated by Prof Ashafa of the Plant Sciences Department at the University of the Free State and the voucher specimen (Alimed/01/2016/QHb) was deposited in the University herbarium. The IUCN policy statement on research concerning plant species at risk of extinction was adhered to and the plant was confirmed not to be near extinction as it was listed as a plant of the least concern according to the red list of plants by South Africa National Biodiversity Institute (SANBI) (*http://redlist.sanbi.org/genus.php?genus=3050*). The leaves were separated from the whole plant, washed under running water, and air-dried at room temperature until the attainment of uniform weight after 4 days. The dried leaf materials were afterward ground into powder using a laboratory blender (Warring Instrument, USA). The acquisition of the *L. montana* aqueous leaf extract according to Ogunyemi et al. (2019) with slight modification was achieved by weighing 2 g of the samples in a 250 mL conical flask and extracted with 200 mL distilled water. The flask containing the mixture was suspended on a heater with a magnetic stirrer (MSH 10, Labcon Consumables, South Africa) (6 *g*) exposed to heat at 65 °C for 4 hours. The cooled mixture was filtered using adsorbent cotton wool followed by Whatman filter paper No 1 and thereafter centrifuged (BHG Roto Uni II, Germany) (650 *g*) for 5 min to collect the supernatant used for the synthesis of ZnONPs.

Synthesis of ZnONPs

One hundred millilitres (100 mL) of zinc oxide (1 M) and freshly generated *L. montana* aqueous leaf extract (ratio 1:1) was mixed in a 200 mL conical flask, subjected to continuous agitation (10 *g*) at 70 °C for 4 hours to obtain NPs solution. The mixture was cooled at room temperature and centrifuged at 10000 *g* for 20 minutes and the residue, NPs pellets were washed four times with distilled water, dried at 50 °C and kept at -80 °C pending further characterisation and analysis (Ogunyemi et al. 2019) while the supernatant was discarded.

Characterisation of NPs

UV-Vis spectrum analysis

The synthesised *Lessertia montana* zinc oxide nanoparticles (LmZnONPs) was characterised (first of all) by measuring and noting the point of optimum absorption using ultra-violet visible (UV) 5 Bio spectrophotometer (Metler Toledo, Switzerland) in the 100 – 800 nm range with aim of evaluating the optical property of the ZnONPs.

Scanning electron microscope (SEM) / energy-dispersive x-ray spectroscopy (EDS)

The synthesised ZnONPs' structural morphology and elemental composition were analysed with the use of SEM combined with energy dispersive spectrum (EDS) using Tescan Vega 3 SEM Oxford X-Max^N EDS equipment. A small quantity of synthesised *L. montana* ZnONPs powder was sparingly sprinkled on the carbon-coated copper grid and thereafter dried under mercury lamp for 10 minutes.

Fourier transform infrared spectroscopy (FT-IR)

Lessertia montana ZnONPs were subjected to the Fourier transform infrared (FTIR) machine, to have an insight about the functional biomolecules embedded in the synthesised NPs and this, was achieved with the aid of Spectrum 100 series FTIR spectrometer (Perkin Elmer, Waltham, Massachusetts, United States). The sample was scanned (4 cm^{-1} resolution) in the spectra or wavelength range of 650-4000 cm^{-1} at room temperature.

X-ray diffraction (XRD)

The D8 advance diffractometer (Bruker AXS, Germany) using a LynxEye detector was used. The voltage set at 40 kV, tube current 40 mA and Cu-Kα radiation ($\lambda K\alpha_1$ = 1.5406Å) was employed providing information about the morphology of the NPs. The recorded range of 2Θ was 20-100 with a 0.5-second/step, equivalent to an effective time of 92 second/step for a scintillation counter. The Debye-Scherrer's formula was used to estimate the crystallite particle sizes.

Antioxidant assays

The free radicals scavenging activities of the synthesised NPs were assessed using DPPH, ABTS, and metal chelating assays.

DPPH radical scavenging activity

The method of Braca et al. (2001) was adopted to determine the reduction of 1, 1-diphenyl-2-picrylhydrazyl (DPPH) radical by *L. montana* ZnONPs and other samples (extract, ZnO and quercetin) at various concentrations (0.125 – 1.000 g/L) prepared in 10% dimethyl sulfoxide (DMSO). Briefly, 0.1 mL of the samples were exposed to 0.1 mL methanolic solution (0.004%) DPPH radical in a 96-well microtiter plate. Subsequently, the inhibition of the DPPH radical by the samples was viewed by the changes in colour from pink to yellow and golden following 30 minutes incubation in the dark. The absorbance was measured at 517 nm. The percentage inhibition of the sample that scavenged DPPH radical was calculated using the expression $[(A_0–A_1)/A_0]\ x\ 100$, where A_0 is the absorbance of the control, and A_1 is the absorbance of the sample. The half-maximal inhibitory concentration (IC_{50}) values of the samples were calculated graphically and accordingly (Balogun and Ashafa 2016a).

ABTS radical determination

The ability of the samples to scavenge $ABTS^+$ chromophore resulting from the reaction of ABTS solution with potassium persulfate was determined based on Re et al. (1999) method. 50 mL of 7 mM aq. ABTS and 2.45 mM $K_2S_2O_7$ (50 mL) were prepared, reacted in the dark for 16 hours to produce an ABTS-$K_2S_2O_7$ solution. Approximately 0.2 mL of the solution was exposed to 0.02 mL aliquot of the sample and absorbance measured after 15 minutes of incubation at 734 nm using a BIO-RAD microplate reader (model 650, Japan).

Metal chelating activity

Dinis et al. (1994) protocol for determining the chelating capacity of a substance was used. One hundred µL *L. montana* ZnONPs and other samples at the tested concentrations were mixed with 0.5 mL 2 mM $FeCl_2$ solution and the reaction began with the addition of 0.2 mL (5 mmol/L) ferrozine, shook vigorously and thereafter allowed to stand at room temperature for 600 seconds. The spectrophotometric measurement of the mixture was taken at 562 nm. The percentage inhibition of ferrozine–Fe^{2+} complex formation was determined from the expression $[(A_0–A_1)/A_0]\ x\ 100$ as described above.

In vitro antidiabetic potentials

The alpha-amylase (α-AML) and alpha-glucosidase (α-GCD) assays were used to assess the antidiabetic activity (*in vitro*) of the green synthesised ZnONPs as presented in the reports of various authors below.

α-Amylase inhibitory assay

McCue and Shetty (2004) modified procedure was adopted in determining the inhibitory effect of α-AML by the *L. montana* zinc oxide nanoparticles. In brief, 50 µL of the samples (ZnONPs, extract, ZnO and acarbose) at ranging concentrations of 0.125 – 1.000 g/L were reacted with the same volume of α-AML prepared in sodium phosphate buffer (SPB; 0.02 M, pH 6.9) at a concentration of 0.5 g/L and pre-incubated at 25 °C for 10 minutes. Subsequently,

the addition of 50 µL of the 1% starch solution into the sample wells followed by 0.1 mL of di-nitro salicylic acid (DNS) reagent to stop the reaction and incubated at 25 °C for another 10 minutes. The mixture was suspended in boiling water for 5 minutes, thereafter cooled, diluted with 1 mL distilled water (DW), and measured the absorbance at 540 nm. Distilled water replaced the extract to represent the control using the same protocol. The α-amylase inhibitory activity was calculated as percentage inhibition following the above expression $[(A_0–A_1)/A_0] \times 100$ and the IC_{50} calculated graphically as defined in the report of Balogun and Ashafa (2016a).

Kinetics of α-amylase inhibition

The mode of α-AML inhibition by *L. montana* ZnONPs was evaluated according to Ali et al. (2006) method. The reaction mixture contained 0.25 mL synthesised ZnONPs (5 mg/mL) pre-incubated with 0.25 mL α- AML solution for 10 minutes at 25 °C in a set of 5 test tubes and 0.25 mL phosphate buffer (PB) pre-incubated with 0.25 mL α-AML in another set of 5 test tubes. Thereafter, 0.25 mL starch solution in increasing concentrations (0.30 – 5.00 gL^{-1}) was dispensed in all test tubes to set the reaction in motion, followed by the introduction of DNS (0.02 mL) to bring the reaction to an end. The protocol continued as described above in the α-amylase inhibitory assay. Moreover, in an effort to determine the amount of reducing sugars released and converted to reaction velocities, a maltose standard curve was plotted, where the kinetics of inhibition of α-AML activity by synthesised ZnONPs was determined using Lineweaver and Burk (1934).

α-Glucosidase inhibitory assay

The antidiabetic effect of the *L. montana* ZnONPs was also assessed on the α-glucosidase enzyme using the procedural description of Kim et al. (2005) where the substrate, p-nitrophenyl glucopyranoside (*p*NPG) (5 mM) used was prepared in 0.02 M phosphate buffer (pH 6.9). Fifty µL of the varying concentrations of the samples (0.125 – 1.000 g/L) pre-incubated with 0.1 mL α-glucosidase (0.5 g/L) were mixed in a test tube. Fifty µL *p*NPG was afterward introduced into the reaction mixture to begin the reaction while 2 mL Na_2CO_3 (0.1 M) was finally dispensed to stop the process followed by incubation at 37 °C for 30 min. The α-glucosidase activity was determined by measuring the yellow-coloured para-nitrophenol (*p*NP) released from *p*NPG at 405 nm as the percentage inhibition determined by adopting the expression $[(A_0–A_1)/A_0] \times 100$ and the IC_{50} obtained as explained in the work of Balogun and Ashafa (2016a).

Mode of α-glucosidase inhibition

Ali et al. (2006) modified method was used to explore the kinetics of inhibition of the enzyme by synthesised ZnONPs. In summary, 0.05 mL (5 g/L) sample was diluted with 0.1 mL of α-GCD solution pre-incubated for 10 minutes at 25 °C in a set of five vials and concurrently, α-GCD solution reacted with 0.05 mL phosphate buffer (pH 6.9) in another set of 5 vials. Subsequently, fifty microliters *p*NPG in ascending concentrations (0.125 – 2.000 g/L) was introduced to the two sets of test vials to kick-start the reaction process and the mixture allowed to incubate at 25 °C for 10 minutes. Finally, the reaction was terminated with 0.5 mL of Na_2CO_3. A para-nitrophenol (*p*-NP) standard was used to depict spectrophotometrically the amount of reducing sugars released and kinetics of *L. montana* ZnONPs on the α-glucosidase activity determined using Michaelis-Menten kinetics.

Statistical analysis

Data analyses were carried out by one-way analysis of variance (ANOVA), followed by Bonferroni's multiple comparison test. Results expressed as mean ± standard error of mean (SEM) using Graph pad Prism version 3.0 for Windows, Graph Pad Software, SanDiego, California, USA.

RESULTS AND DISCUSSION

The simplicity, stability, affordability, and eco-friendliness of the synthesised NPs from medicinal plants afford great relevance to the biological methods in nanotechnology, hence the acceptability in drug discovery and development (Sun et al. 2019). The antioxidant and antihyperglycaemic potentials of the aqueous leaf extract of *Lessertia montana* (Alimi and Ashafa 2017) propelled undertaking the study to evaluate the effect of the synthesised nanoparticle (*Lessertia montana* ZnONPs) on these disease conditions. In the work of Alimi and Ashafa (2017), various phytochemicals such as alkaloids, flavonoids, phenols, saponins, etc. are detected in the aqueous extract of the leaf and in fact, these phytoconstituents are regarded as polyphenols (Ezealisiji et al. 2019) and also depicted by the various functional groups on the FTIR spectrum. Therefore, the probable mechanism of ZnONPs synthesis from *L. montana* entails the reaction of Zn^{2+} in the solution with the polyphenols (flavonoids, alkaloids, phenols) in the extract resulting in the reduction of the Zn^{2+} to ZnO, which on complexation will (at the end of the reaction) form ZnONPs (Basneth et al. 2018; Ogunyemi et al. 2019; Ezealisiji et al. 2019).

The zinc oxide nanoparticles synthesised using *L. montana* leaves extract was observed to give a light-yellow precipitate, dried to obtain ZnO nanopowder used in the characterisation processes (CP). The CP was initiated with a UV-Vis spectrophotometer to determine

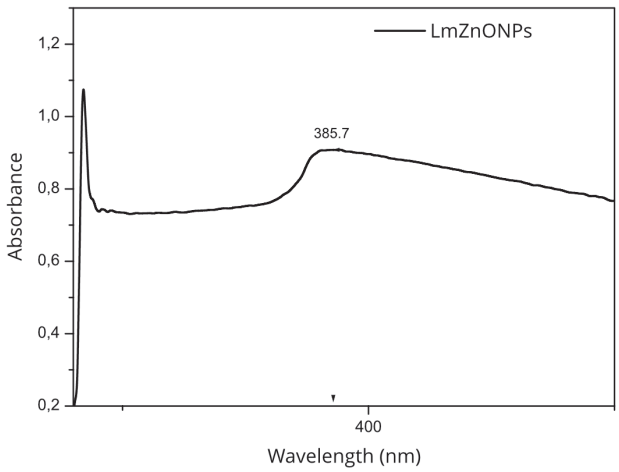

Figure 1. UV-Vis spectra of synthesised *L. montana* ZnONPs showing the maximum absorbance at 387.5 nm.

the region of optimum absorption of the ZnONPs (Fig. 1) observed at a wavelength range of 387.5 nm (Fig. 1) after being monitored on the spectra range between 100 - 800 nm. The observed absorbance value aligned with the reports of previous authors who submitted the maximum absorption of ZnO to be in 380-387 range (Nithya and Kalyanasundharam 2018; Mohammadian et al. 2018; Ogunyemi et al. 2019). However, it must be noted that the differences in the absorption of a substance and in this case, ZnO nanoparticle is dependent on several factors including synthesis procedure, particle size, shape, contamination, and so on. Intriguingly, the observed absorption of *L. montana* ZnONPs at 387 nm was in line with the submission of Nithya and Kalyanasundharam (2019) for *C. halicacabum* leaf. Additionally, the energy of the bandgap was calculated from the expression $E = h\nu = hf = hc/\lambda$ since $f = c/\lambda$

Where 'h' denotes the Plank's constant, 'c' signify the speed of light while 'λ' connotes the wavelength

The optical band gap energy for *L. montana* ZnONPs was calculated to be 3.2 eV. It is worthy of mention that different studies have reported different values for ZnONPs. In a study, it is submitted at 3.88 eV (Ogunyemi et al. 2019), whereas other reports maintained that it varies between 3.1 to 3.3 eV (Srikant and Clarke, 1998) and 3.16 - 3.22 eV (Ramesh et al. 2014; Rehana et al. 2017) while others (Vishnukumar et al. 2018; Kalpana and Devi Rajeswari 2018) established it at 3.3 eV and 3.37 eV, respectively. However, variation in band gap energy has been suggested to be due to valence band-donor transition overpowering the optical absorption (Srikant and Clarke 1998). The obtained value for the study was in agreement with the report of Ramesh et al. (2014).

Fourier transform infrared spectroscopy was performed on the synthesised ZnONPs with the view to depict the likely functional groups or the phytochemicals acting as capping and stabilizing agents. FTIR was similarly undertaking to express the vibrational and rotational motion of the concerned molecule. Thus, the FTIR spectrum for *L. montana* ZnONPs revealed a peak at 3365 cm^{-1} corresponding to the O-H stretching of hydroxyl groups. Bayrami et al. (2020) citing from the work of Sundrarajan et al. (2015) submitted that peaks in the region of 3700 to 3300 are due to O-H stretching vibration. Peaks at 2945 cm^{-1}, 1412 cm^{-1} 1046 cm^{-1} corresponded to broad bands of medium C-H (Bayrami et al. 2020), strong C-C and strong, broad CO-O-CO stretching due to alkanes, aromatic group (Elumalai et al. 2015; Rehana et al. 2017), and anhydride respectively. The peak at 1596 cm^{-1} corresponds to medium N-H bending due to amine region, 892 cm^{-1} corresponded to strong C=C bending due to alkene (vinylidene) and 699 cm^{-1} due to strong C=C bending due to alkene (cis disubstituted) (Fig. 2). The reports of Alimi and Ashafa (2017), as well as Ashafa et al. (2019), reported various phytochemicals such as alkaloids, flavonoids, phenolics, tannins, triterpenes, phytosterols, and cardiac glycosides. Interestingly, most of these functional groups observed in the FTIR spectra underlie these phytochemicals. Typically, alkaloids contain nitrogen groups such as amide; phenols and flavonol (a class of flavonoids) bear OH groups attached to the aromatic ring structures. In line with the aforementioned, the presence of these functional groups in the spectrum is indicative that these secondary metabolites bond strongly to ZnONPs despite several washing, hence, the possible association between the phytoconstituents and surface of the Zn resulting in the potential conversion of ZnO

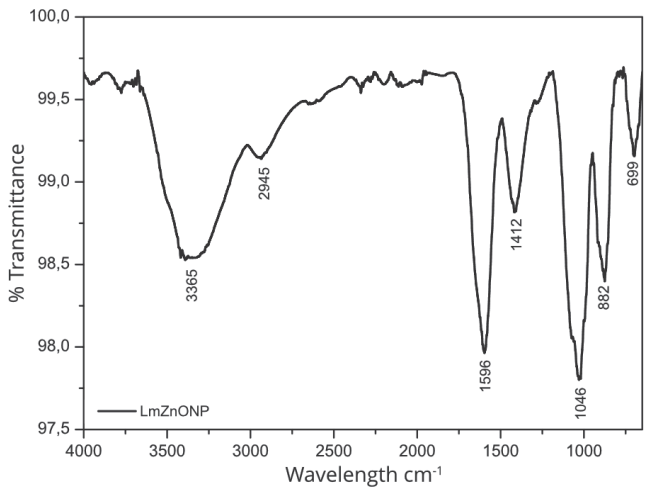

Figure 2. Fourier transform infrared (FTIR) spectra of *L. montana* ZnONPs showing various prominent peaks.

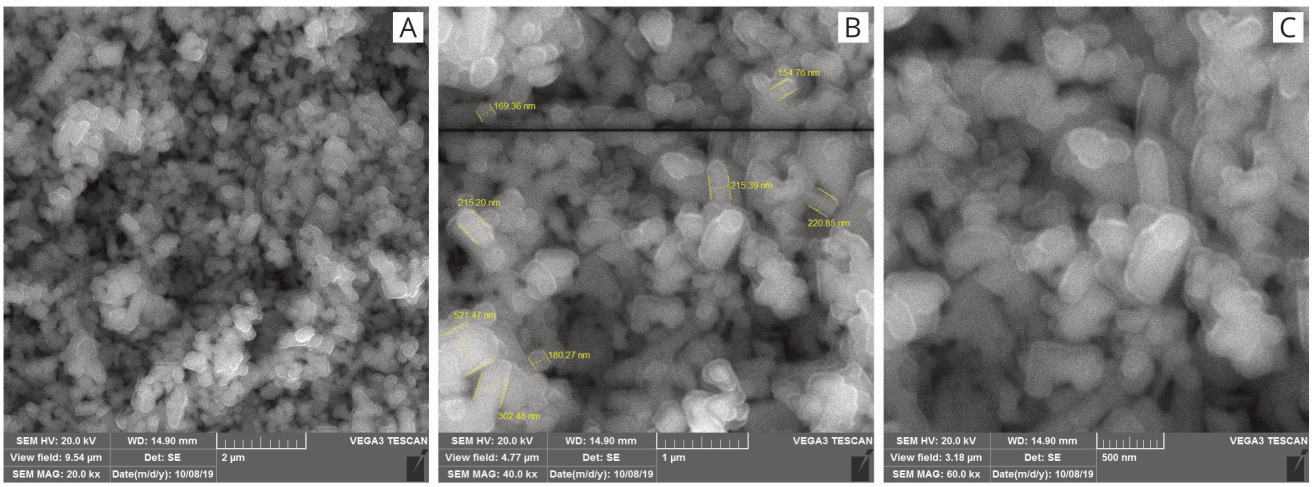

Figure 3. A, B and C are SEM pictures of synthesised *L. montana* ZnONPs at 2 µm, 1 µm and 500 nm, respectively.

to ZnONPs while maintaining the stability of ZnONPs (Rajakumar et al. 2018).

The use of the SEM technique on a substance accords information on the morphology of the substance and in our case, the synthesised ZnO nanostructures. In the present study, a critical view of the NPs morphology indicated a mixture of cubical and spherical structures which was in agreement with the work of Rajakumar et al. (2018) though the presence of the cubic-like structures were more (Fig. 3A, 3B and 3C) with varying size ranging from 154.78 to 521.47 nm (Fig. 3B). The energy dispersive spectra (EDS) provided details on the composition of the elements, i.e. zinc and oxygen involved in the compound ZnO or the stoichiometric ratio, found to be 82.6 and 17.4 proportion respectively in this study (Fig. 4). The observed revelation is indicative of the usage of an analytical grade of zinc oxide (chemical) powder (Kumar et al. 2013; Ogunyemi et al. 2019) for the *L. montana* ZnONPs synthesis. Interestingly, the EDS spectrum showed the presence of other elements including nitrogen and carbon, which could be attributed to the endowed bioactive constituents available in *L. montana* plant and responsible for the stabilization of ZnONPs as established in the report of Bala et al. (2015).

Fig. 5 showed prominent peaks (arising from ZnO) positioned at various 2Θ values 31.8, 34.4, 36.3, 47.5, 56.6, 62.9, 66.4, 68.0, 69.1, 72.6, 77.0 and 81.4 degrees which correspond to 'hkl'(miller indices) crystal planes of 100, 002, 101, 102,110, 103, 200, 112, 201, 004, 202 and 104, respectively. The Scherer equation adopted to evaluate the green synthesised ZnONPs crystallite size as shown in the expression below:

$$D = K\lambda/\beta Cos\Theta$$

Where D represent the crystallite size, K is the shape factor (constant) and equals 0.94, λ is the x-ray wavelength (1.5406Å) and β is the full width at half maximum of the dominant or peak of interest. Thus, the D values for the *L. montana* ZnONPs visible peaks are 27.3, 24.8, 23.3, 14.7, 11.6, 8.6, 7.3, 11.0, 9.6, 11.3, 7.9 and 8.6 nm, respectively. These values (sizes) are smaller as compared to the SEM (larger size) report, attributed to the agglomeration of the smaller size particles (Ogunyemi et al. 2019) particularly if the synthesis occurs in an aqueous medium (Rajakumar et al. 2018) as achieved in this study. The crystallite sizes ranged between 7.3 to 27.3 nm with an average size of

Table 1. Free radicals potentials and metal chelating effect of synthesised *L. montana* ZnONPs.

Parameters	IC_{50} (g/L)			
	L. montana ZnONPs	*L. montana*	ZnO	Quercetin
DPPH	$0.120 \pm 1.42^{a*}$	0.261 ± 1.55^{b}	1.165 ± 5.60^{c}	0.349 ± 4.27^{d}
ABTS	0.711 ± 8.07^{a}	0.964 ± 7.27^{b}	1.166 ± 9.45^{c}	0.093 ± 3.77^{d}
Metal chelating	0.184 ± 5.94^{a}	0.554 ± 3.00^{b}	0.591 ± 3.15^{c}	0.027 ± 9.87^{d}

ZnONPs: zinc oxide nanoparticles; DPPH: 1,1-diphenyl-2-picrylhydrazyl; ABTS: 2,2-azino benzothiazolidine(-6-sulphonic) acid; ZnO: zinc oxide
*Values with different superscript letters along the same column for each parameter are significantly different ($p < 0.05$) from each other

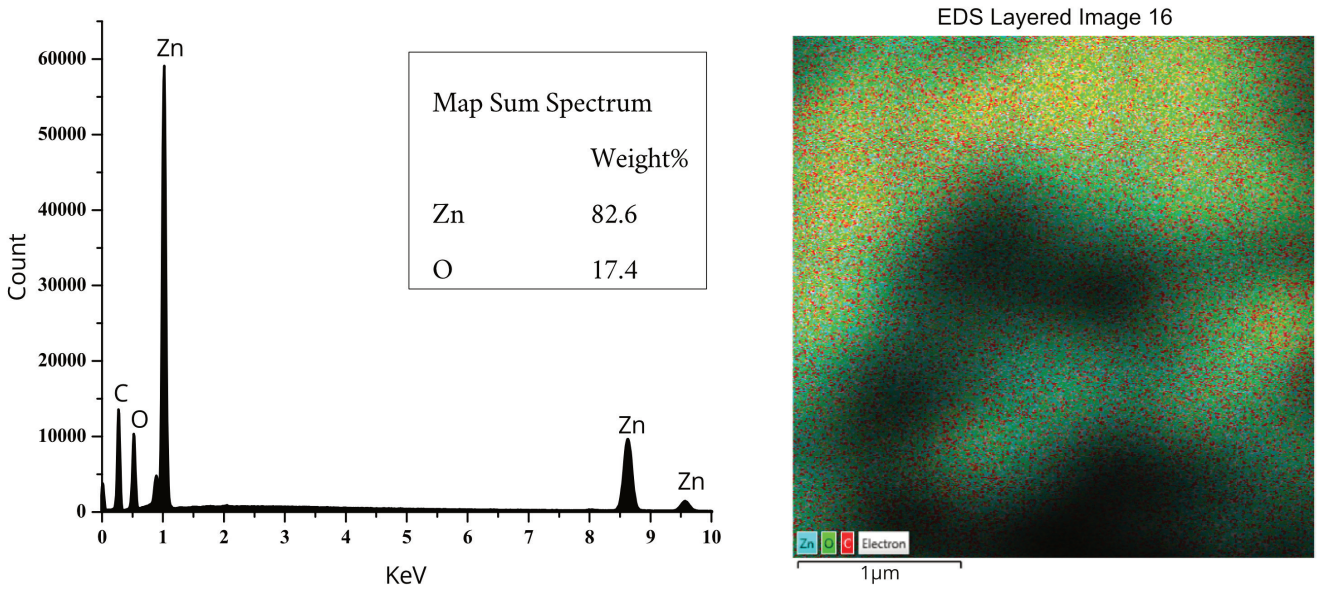

Figure 4. Energy dispersive spectra (EDS) of the synthesised *L. montana* ZnONP showing the elemental composition of ZnO in the nanostructures (left) and the corresponding image (right).

13.8 nm. Interestingly, very few studies on ZnO using medicinal plants have this type of very small nano-sized particles. Smaller-sized nanoparticles are endowed with larger surface area to volume ratio, which enhances their binding to cell's surface, according them a great deal of preference in biological applications (Rehana et al. 2017; Vishnukumar et al. 2019).

The negative consequences of free radicals have necessitated research into this field (free radical chemistry). Free radicals (FRs) are reactive oxygen or nitrogen species produced by the body on exposure to diseased state (Lobo et al. 2010). It must be noted that FRs are not necessarily bad but excessive production in the body system is what must be guided against. Hence, equilibrium between FRs and the body's antioxidant defence mechanism must be maintained for the proper functioning of the cells, otherwise, it results in a state of oxidative stress, which means the defence mechanism of the body is overpowered or compromised and ultimately result into cell death. Thus, prompt intervention with the use of antioxidants (synthetic or natural) is necessary (Balogun and Ashafa 2016b). In an effort to study the effect of antioxidative substances on free radicals, various *in vitro* (DPPH, ABTS, hydroxyl radicals, superoxide anions, etc.) and *in vivo* methods are adopted by researchers. In this study, the antioxidative potential of the synthesised NPs was evaluated on DPPH and ABTS as well as metal chelating. It was observed that going by half-maximal inhibitory concentration results, *L. montana* ZnONPs performed exceedingly well ($p < 0.05$) in all the assays including DPPH (120.31 µg/mL), ABTS (711.45 µg/mL) and metal chelating (184.16 µg/mL) when compared with other samples (extract, ZnO and quercetin) except with ABTS and metal chelating where the control, quercetin displayed better ($p < 0.05$) activity (93.94, 27.81 µg/mL, respectively) which is expected (Table 1). The excellent activity observed by synthesised ZnONPs against DPPH as reflected in the colour change from pink to yellow is an indication of its potential in reducing stable DPPH with its hydrogen ion donating-ability. DPPH method is the most important assay for the determination of the antioxidant potential of a substance or compound (followed by ABTS assay) (Sanchez-Moreno et al. 1999; Sagar and Ashok 2012). The mechanism of action is that the antioxidant substance donates hydrogen atom to the radical (DPPH) with an

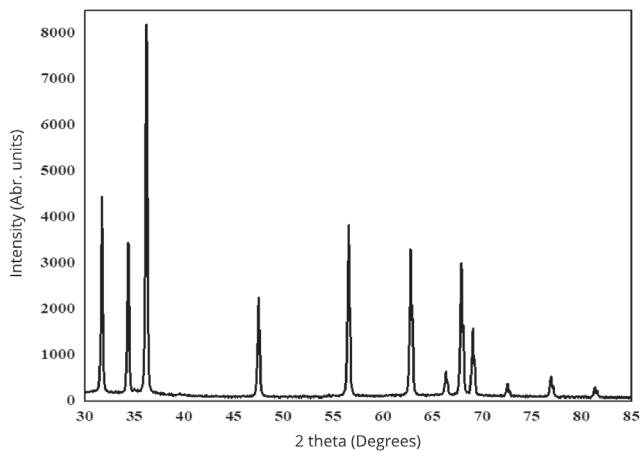

Figure 5. XRD spectrum of synthesised *L. montana* ZnONPs.

Table 2. Inhibitory activities of synthesised *L. montana* ZnONPs on hydrolysing enzymes of carbohydrates.

Parameters	IC_{50} (g/L)			
	L. montana ZnONPs	*L. montana*	ZnO	Acarbose
α-amylase	0.620 ± 3.35[a]*	0.196 ± 3.39[b]	0.300 ± 5.37[c]	0.594 ± 1.48[d]
α-glucosidase	0.037 ± 7.48[a]	0.095 ± 7.38[b]	0.119 ± 4.23[c]	0.065 ± 5.38[d]

ZnONPs: Zinc oxide nanoparticles; ZnO: Zinc oxide.
*Values with different superscript letters along the same column for each parameter are significantly different ($p<0.05$) from each other

unbalanced shell electron, resulting in the reduction or reduced form of the radical, and when this is achieved, the pink colour of the radical changes to yellow. Summarily, since the introduction of antioxidant substance cushions or fortifies the weakened defence mechanism preventing cell death (Lewinski et al. 2008; Lobo et al. 2010), *L. montana* ZnONPs may be suggested to exhibit a similar role. Interestingly, these findings corroborate the reports of similar studies where synthesised ZnONPs from medicinal plants inhibits the activities of the studied radicals. Typically, the activity of *Costus igneus* aqueous leaf (20-100 μg/mL) extracts was compared with Ci-ZnO (nanoparticle) against DPPH and was found to depict 75% inhibition as compared with extract alone having 55% (Vinotha et al. 2019). Additionally, in a study by Rehana et al. (2017), where the free radical scavenging potentials of five plants (*A. indica*, *H. rosa-sinensis*, *M. koenigi*, *M. oleifera*, and *T. indica*) used in the synthesis of ZnONPs were tested against ABTS, DPPH, hydroxyl radical, superoxide radical and hydrogen peroxide revealed significant activities better than standards (ascorbic acids and rutin) (Rehana et al. 2017). A similar trend was also reported in the work of Rajakumar et al. (2018) with *Andrographis paniculata* leaf ZnONPs curbing the activities of DPPH, reducing power and nitric oxide.

Diabetes mellitus is a chronic metabolic disease characterised by hyperglycaemia due to abnormalities in protein, carbohydrate, and lipids metabolism resulting from ineffective insulin or insulin-resistant or both (Krentz and Bailey 2005; Rehana et al. 2017). During postprandial hyperglycaemia, the utmost management approach of the ailment is to inhibit the constant production of glucose (available in the blood) aided by hydrolysing enzymes such as alpha-amylase (found in the pancreas) and alpha-glucosidase (found in the brush border of the intestine) (Balogun and Ashafa 2017). Notable inhibitors of these enzymes are acarbose, miglitol, and so on, which act by slowing down the persistent hydrolysis of starch to produce glucose. Sadly, these inhibitors come with side effects such as gastrointestinal (GIT) discomfort, bloating, etc., hence, looking for an alternative inhibitor from natural products without side effects becomes germane (Sathya and Siddhuraju 2012; Rehana et al. 2017). Moreover, it is important to state that any inhibitor with this feature must be able to inhibit alpha-amylase mildly while inhibiting alpha-glucosidase strongly. A view of the antidiabetic result from the study showed that the *L. montana* aqueous extract (0.197 g/L) and synthesised ZnONPs (0.037 g/L) revealed the best potential at significantly ($p < 0.05$) inhibiting the activities of α-amylase and α-glucosidase respectively when compared with other samples and standard, acarbose (0.594 and 0.065 g/L, respectively). Intriguingly, as reiterated above, *L. montana* ZnONPs showed a character depicted of a good antihyperglycaemic agent with the lowest IC_{50} value (0.037 g/L) against alpha-glucosidase (strongest inhibition) and highest IC_{50} value (0.620 g/L) against alpha-amylase (mildest inhibition) (Table 2). The result is in tandem with the revelation from Rehana et al. (2017) where *T. indica* ZnONPs exhibited the highest inhibitory concentration against alpha-amylase and alpha-glucosidase enzymes as compared with other four plants, whose inhibitions are better than ZnONPs synthesised by chemical method. Moreover, too, ZnONPs synthesised by *A. paniculata* revealed a moderate alpha-amylase activity, which was better than the extract counterpart (Rajakumar et al. 2018).

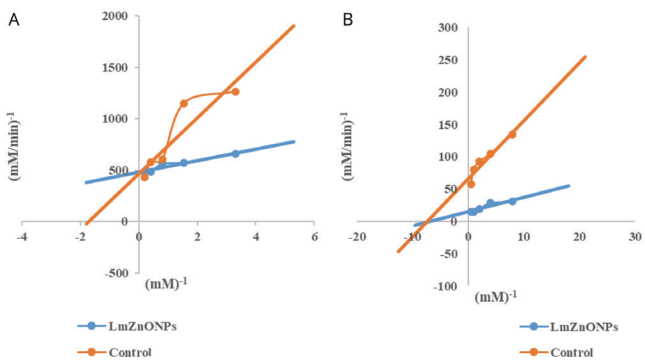

Figure 6. A competitive inhibition of alpha-amylase (A) and non-competitive inhibition of alpha-glucosidase (B) by *L. montana* ZnONPs.

In this study, the likely mode of inhibition for α-amylase by *L. montana* ZnONPs established a constant Vmax value

(0.0021 mM/min) between the control and NPs with a decreased Km values from 0.579 mM^{-1} (control) to 0.116 mM^{-1} (*L. montana* ZnONPs) signifying a competitive inhibition (Fig. 6A). The implication of this is that synthesised *L. montana* ZnONPs competed with the substrate at binding at the active site of the enzyme, thus slowing down the conversion of carbohydrate to disaccharides. On the other hand, a constant Km value (0.14 mM^{-1}) and a decreased Vmax values from 0.066 mM/min to 0.015 mM/min for alpha-glucosidase thus, depicting a non-competitive inhibition (Fig. 6B). This thus indicates that *L. montana* ZnONPs possibly binds to a site apart from the active site of the enzyme thereby binding with either free enzyme or enzyme-substrate complex interfering with the action of both (Mayur et al. 2010).

CONCLUSION

The *Lessertia montana* synthesised zinc oxide nanoparticles, no doubt, revealed good antioxidative and antidiabetic potentials which could be attributed to the presence of phytonutrients. Hence, the need to embrace plant-derived nanoparticles becomes vital, not only because of its low cost of synthesis, environment friendliness etc. but owing to the enhanced activity as compared with the bulk extract (as depicted in this study). Furthermore, the relatively small size of NPs, which would aid effective absorption or penetration into cells, including possible interaction with the cell surface of biomolecules in order to elicit adequate cellular responses would be preferable for biological applications.

ACKNOWLEDGMENTS

The authors acknowledge the support from Directorate Research and Development, University of the Free State (UFS), Free State for the postdoctoral fellowship awarded to Dr. FO Balogun (2-459-B3425) tenable at Phytomedicine and Phytopharmacology Research Group, Department of Plant Sciences, UFS, Qwaqwa Campus, Free State. The authors also acknowledge the intellectual input of Dr. Obi of Physics Department, UFS, Qwaqwa, Free State in the interpretation of some of the results as well as National Research Foundation (NRF) for the usage of Tescan Vega 3 SEM Oxford X-Max^N EDS equipment (provided to Chemistry Department, UFS, Qwaqwa) for paid SEM-EDS analyses.

REFERENCES

Aboyade OM, Styger G, Gibson D, Hughes G (2014) *Sutherlandia frutescens*: the meeting of science and traditional knowledge. J Altern Complement Med 20(2):71-76.

Ali H, Houghton PJ, Soumyanath A (2006) Alpha-amylase inhibitory activity of some Malaysian plants used to treat diabetes; with particular reference to *Phyllanthus amarus.* J Ethnopharmacol 107(3):449-455.

Alimi AA, Ashafa AOT (2017) An *in vitro* evaluation of the antioxidant and antidiabetic potential of *Sutherlandia montana* E. Phillips & R.A. Dyer leaf extracts. Asian Pac J Trop Biomed 7(9):765-772.

Ashafa AOT, Balogun FO, Adegbegi JA (2019) *In vitro* kinetics of inhibition of the endogenous hyperglycaemia antagonists of alpha-amylase and alpha-glucosidase in the pod and seed extracts of *Lessertia montana*. J Appl Pharm Sci 9(01):42-50.

Bala N, Saha S, Chakraborty M, Maiti M, Das S, Basu R, Nandy P (2015) Green synthesis of zinc oxide nanoparticles using *Hibiscus subdariffa* leaf extract: effect of temperature on synthesis, anti-bacterial activity and anti-diabetic activity. RSC Adv 5:4993–5003.

Balogun FO, Ashafa AOT (2017) Aqueous roots extract of *Dicoma anomala* (Sond.) extenuates postprandial hyperglycaemia *in vitro* and its modulation against on the activities of carbohydrate-metabolizing enzymes in streptozotocin-induced diabetic Wistar Rats. S Afr J Bot 112:102-111.

Balogun FO, Ashafa AOT (2016a) Antioxidants, hepatoprotective and ameliorative potentials of aqueous leaf extract of *Gazania krebsiana* (Less.) against carbon tetrachloride –induced liver injury in rats. Trans Royal Soc S Afr 71(2):145-156.

Balogun FO, Ashafa AOT (2016b) Antioxidant and hepatoprotective activities of aqueous root extracts of *Dicoma anomala* (Sond.) against carbon tetrachloride induced liver damage in rats. J Trad Chin Med 36:505-513.

Basnet P, Chanu TI, Samanta D, Chatterjee S (2018) A review on bio-synthesized zinc oxide nanoparticles using plant extracts as reductants and stabilising agents. J Photochem Photobiol B Biol 183:201-221.

Bayrami A, Haghgooie S, Pouran SR, Arvanag FM, Habibi-Yangjeh A (2020). Synergistic antidiabetic activity of ZnO nanoparticle encompassed by *Urtica dioica* extract. Adv Powder Technol 31:2110-2118.

Braca A, Tommasi ND, Bari LD, Pizza C, Politi M, Morelli I (2001) Antioxidant principles from *Bauhinia terapotensis.* J Nat Prod 64(7):892-895.

Dinis TCP, Madeira VMC, Almeida LM (1994) Action of phenolic derivatives (acetoaminophen, salycilate and 5-aminosalycilate) as inhibitors of membrane lipid

peroxidation and as peroxyl radical scavengers. Arch Biochem Biophys 315(1):161-169.
Elumalai K, Velmurugan S, Ravi S, Kathiravan V, Ashokkumar S (2015) Bio-fabrication of zinc oxide nanoparticles using leaf extract of curry leaf (*Murraya koenigii*) and its antimicrobial activities. Mat Sci Semicon Process 34:365-372.
Ezealisiji KM, Siwe-Noundou X, Maduelosi B, Nwachukwu N, Krause RWM (2019) Green synthesis of zinc oxide nanoparticles using *Solanum torvum* (L.) leaf extract and evaluation of the toxicological profile of the ZnO nanoparticles-hydrogel composite in Wistar albino rats. Int Nano Let 9:99-107
Fakhari S, Jamzad M, Fard HK (2019) Green synthesis of zinc oxide nanoparticles: a comparison. Green Chem Lett Rev 12(1):19-24.
Kalpana VN, Devi Rajeswari V (2018) A review on green synthesis, biomedical applications and toxicity studies of ZnONPs. Bioinorganic Chem Appl 18:3569758.
Kim YM, Jeong YK, Wang MH, Lee WY, Rhee HI (2005) Inhibitory effects of pine bark extract on alpha-glucosidase activity and postprandial hyperglycemia. Nutr 21(6):756-761.
Krentz AJ, Bailey CJ (2005) Oral antidiabetic agents: current role in type 2 diabetes mellitus. Drugs 65(3):385-411.
Kumar SS, Venkateswarlu P, Rao VR, Gollapalli NR (2013) Synthesis, characterization and optical properties of zinc oxide nanoparticles. Int Nano Lett 3:30-36.
Lewinski N, Colvin V, Drezek R (2008) Cytotoxicity of nanoparticles. Small 4:26-49
Lineweaver H, Burk D (1934) The determination of enzyme dissociation constants. J Am Chem Soc 56(3):658-666.
Lobo V, Patil A, Phatak A, Chandra N (2010) Free radicals, antioxidants, and functional foods: Impact on human health. Pharmacog Rev 4(8):118-126.
Mayur B, Sandesh S, Shruti S, Sung-Yum S (2010) Antioxidant and α- glucosidase inhibitory properties of *Carpesium abrotanoides* L. J Med Plant Res 4:1547-1553.
Mccue P, Shetty K (2004) Inhibitory effects of rosmarinic acid extracts on porcine pancreatic amylase *in-vitro*. Asia Pac J Clin Nutr 13(1):101-106.
Mohammadian M, Es'haghi Z, Hooshmand S (2018) Green and chemical synthesis of zinc oxide nanoparticles and size evaluation by UV-vis spectroscopy. J Nanomed Res 1:7.
Nithya K, Kalyanasundharam S (2019) Effect of chemically synthesis compared to biosynthesized ZnO nanoparticles using aqueous extract of *C. halicacabum* and their antibacterial activity. OpenNano 4:100024.
Ogunyemi SO, Abdallah Y, Zhang M, Fouad H, Hong X, Ibrahim E, Islam Masum MdM, Hossain A, Mo J, Li B (2019) Green synthesis of zinc oxide nanoparticles using different plant extracts and their antibacterial activity against *Xanthomonas oryzae* pv oryzae. Artif Cells Nanomed Biotechnol 47(1):341-352
Prashanth GK, Prashanth PA, Nagabhushana BM, Ananda S, Krishnaiah GM, Nagenda HG, Sathyananda HM, Rajendra Singh C, Yogisha S, Anand S, Tejabhiram Y (2018) Comparison of anticancer activity of biocompatible ZnO nanoparticles prepared by solution combustion synthesis using aqueous leaf extracts of *Abutilon indicum*, *Melia azedarach* and *Indigofera tinctoria* as biofuels. Artif Cells Nanomed Biotechnol 46:968-979.
Rai M, Ingle A (2012) Role of nanotechnology in agriculture with special reference to management of insect pests. Appl Microbiol Biotechnol 94:287-293.
Rajakumar G, Thiruvengadam M, Mydhili G, Gomathi T, Chung I (2018) Green approach for synthesis of zinc oxide nanoparticles from *Andrographis paniculata* leaf extract and evaluation of their antioxidant, anti-diabetic, and anti-inflammatory activities. Bioprocess Biosyst Eng 41:21-30.
Ramesh M, Anbuvannan M, Viruthagiri G (2014) Green synthesis of ZnO nanoparticles using Solanum nigrum leaf extract and their antibacterial activity. Spectrochim Acta A 136:864-870.
Re R, Pellegrini N, Proteggente A (1999) Antioxidant activity applying an improved ABTS radical cation decolorisation assay. Free Rad Bio Med 26(9-10):1231-1237.
Rehana D, Mahendiran D, Kumar RS, Rahiman AK (2017) *In vitro* antioxidant and antidiabetic activities of zinc oxide nanoparticles synthesized using different plant extracts. Bioprocess Biosyst Eng 40:943-957.
Sagar G, Ashok B (2012) Green synthesis of silver nanoparticles using *Aspergillus niger* and its efficacy against human pathogens. Eur J Expt Biol 2(5):1654-1658.
Sanchez-Moreno C, Larrauri JA, Saura-Calixto F (1999) Free radical scavenging capacity and inhibition of wines, grape juices and related polyphenolic constituents. Food Res Int 32:407-412.
Sangeetha G, Rajeshwari S, Venckatesh R (2011) Green synthesis of zinc oxide nanoparticles by *Aloe barbadensis* Miller leaf extract: structure and optical properties. Mat Res Bull 46:2560-2566.
Sathya A, Siddhuraju P (2012) Role of phenolics as antioxidants, biomolecule protectors and as antidiabetic factors—evaluation on bark and empty pods of *Acacia auriculiformis*. Asian Pac J Trop 5:757-765.
Sorescu A, Alexandrina N, Rodica-Mariana I, Ioana-Raluca S (2016) Green synthesis of silver nanoparticles using plant extracts. Proceed 4th Int Virtual Confer Adv Sci Res; 2016 June 6-10; Chem Sci; Royal Society of Chemistry, Cambridge, UK, 188-193.
Srikant V, Clarke DR (1998) On the optical band gap of zinc oxide. J Appl Phys 83(10):5447-5451.
Sun B, Hu N, Han L, Pi Y, Gao Y, Chen K (2019) Antican-

cer activity of green synthesised gold nanoparticles from *Marsdenia tenacissima* inhibits A549 cell proliferation through the apoptotic pathway. Artif Cells Nanomed Biotechnol 47(1):4012-4019.

van Wyk BE, Albrecht C (2008) A review of the taxonomy, ethnobotany, chemistry and pharmacology of *Sutherlandia frutescens* (Fabaceae). J Ethnopharmacol 119:620-629.

Vinotha V, Iswarya A, Thaya R, Govindarajan M, Alharbi NS, Kadaikunnan S, Khaled JM, Al-Anbr MN, Vaseeharan B (2019) Synthesis of ZnO nanoparticles using insulin-rich leaf extract: Antidiabetic, antibiofilm and antioxidant properties. J Photochem Photobiol 197:111541.

Vishnukumar P, Vivekanandhan S, Misra M, Mohanty AK (2019) Recent advances and emerging opportunities in phytochemical synthesis of ZnO nanostructures. Mat Sci Semicon Proc 80:143-161.